

Magnetism of carbon doped Mn_5Si_3 and Mn_5Ge_3 films

C SÜRGER^{a,*}, K POTZGER^b and G FISCHER^a

^aPhysikalisches Institut, Universität Karlsruhe, D-76128 Karlsruhe, Germany

^bInstitute for Ion Beam Physics and Materials Research, Forschungszentrum Dresden-Rossendorf, D-01328 Dresden, Germany

e-mail: christoph.suerger@pi.uka.de

MS received 12 August 2008; revised 3 March 2009

Abstract. The magnetic properties of $\text{Mn}_5\text{Si}_3\text{C}_x$ and $\text{Mn}_5\text{Ge}_3\text{C}_x$ films prepared by magnetron co-sputtering or C^+ -ion implantation are studied. The carbon-doped films exhibit ferromagnetic properties with Curie temperatures T_C well above room temperature and metallic conductivity, making them possible candidates for future magnetic semiconductor-based devices. In $\text{Mn}_5\text{Si}_3\text{C}_x$, the carbon gives rise to a lattice expansion and a concomitant change of the magnetic order from antiferromagnetic Mn_5Si_3 to ferromagnetic $\text{Mn}_5\text{Si}_3\text{C}_{0.8}$ with $T_C = 350$ K. Likewise, T_C of ferromagnetic Mn_5Ge_3 is strongly enhanced in $\text{Mn}_5\text{Ge}_3\text{C}_{0.8}$. However, in this case the lattice is slightly compressed by carbon. This demonstrates that the effect of carbon on the magnetic behaviour in these compounds is not simply due to a change of the various interatomic distances by carbon but also due to a modification of the electronic band structure.

Keywords. Mn compounds; magnetic films; carbon doping; ion implantation.

1. Introduction

Mn-Si and Mn-Ge compounds exhibit interesting magnetic properties arising from competing magnetic interactions that can lead to ferro-, ferri-, or antiferromagnetic order. It was previously reported that antiferromagnetic Mn_5Si_3 can be driven into a ferromagnetic (or ferrimagnetic) state by insertion of carbon atoms into the voids of Mn octahedra of the hexagonal structure.¹ In particular, magnetron-sputtered $\text{Mn}_5\text{Si}_3\text{C}_x$ films with $x = 0.8$ have a Curie temperature $T_C = 350$ K (refs 2, 3) well above room temperature and even higher than $T_C = 304$ K reported for ferromagnetic Mn_5Ge_3 (ref. 4). Likewise, T_C is enhanced in $\text{Mn}_5\text{Ge}_3\text{C}_x$ films with a maximum $T_C = 442$ K (ref. 5). In an alternative approach to co-sputtering of Mn, Si or Ge, and C from elemental targets, ferromagnetic $\text{Mn}_5\text{Si}_3\text{C}_{0.8}$ and $\text{Mn}_5\text{Ge}_3\text{C}_{0.8}$ can be obtained by ion implantation of carbon into antiferromagnetic Mn_5Si_3 or ferromagnetic Mn_5Ge_3 (ref. 6). The carbon-implanted samples exhibit magnetic properties very similar to their respective co-sputtered counterparts as inferred from resistivity and magnetization measurements. In addition, both carbon-doped compounds show a metallic behaviour in the temperature dependence of the resistivity.^{3,6}

Hence, carbon doping of Mn_5Si_3 or Mn_5Ge_3 may provide a favourable way to fabricate ferromagnetic silicide or germanide films for technological applications because of the easy implementation of these compounds into the semiconductor device fabrication process.⁷ In this paper we will summarize our recent work on the structural and magnetic properties of $\text{Mn}_5\text{Si}_3\text{C}_x$ and $\text{Mn}_5\text{Ge}_3\text{C}_x$ films.

2. Experimental

400 nm thick $\text{Mn}_5\text{Si}_3\text{C}_x$ and $\text{Mn}_5\text{Ge}_3\text{C}_x$ ($x = 0-1$) films were deposited by magnetron sputtering at elevated substrate temperatures of 400–500°C on sapphire substrates as described earlier.^{2,5} Each film was protected by 5–10 nm Si or Ge to avoid oxidation in ambient air. Films with $x = 0$ were implanted with C^+ -ions in three steps of 195, 100, and 45 keV energy.⁶ The respective ion doses were 13, 7.2, and $4.8 \times 10^{16} \text{ cm}^{-2}$ to yield $\text{Mn}_5\text{Si}_3\text{C}_{0.8}$ and 16, 7.2, and $4.8 \times 10^{16} \text{ cm}^{-2}$ to yield $\text{Mn}_5\text{Ge}_3\text{C}_{0.8}$. During implantation the films were heated to the same substrate temperature as applied during sputter deposition of the virgin films.

3. Results and discussion

Figure 1 shows the unit cell of the hexagonal Mn_5Si_3 structure (space group $P6_3/mcm$) which contains

*For correspondence

four Mn_I atoms at positions $4(d)$ ($1/3, 2/3, 0$), six Mn_{II} atoms at positions $6(g)$ ($y_{Mn}, 0, 1/4$) with $y_{Mn} = 0.2358$, and six Si atoms at positions $6(g)$ ($y_{Si}, 0, 1/4$) with $y_{Si} = 0.5991$. For the carbon doped samples previous structural analysis suggests that the carbon is incorporated into the interstitial voids at position $2(b)$ ($0, 0, 0$) of the Mn_{II} octahedra up to a C concentration $x = 0.22$ (ref. 1). Such phases with filled $D8_8$ structure are usually denoted as ‘Nowotny phases’. The binding of impurity atoms such as C, N, and O into the octahedral cavities of the Mn_5Si_3 -type structure has been established for different compounds and is still a topic of current research in materials science and chemistry.⁸ For instance, in some isostructural R–Ge–C (R = Ce, Pr, Nd) alloys an ordered superstructure of one interstitial C atom per three R_5Ge_3 unit cells is formed⁹. In $Mn_5Si_3C_{0.8}$, the shift of the x-ray diffraction lines to lower diffraction angles directly shows that the hexagonal lattice expands with increasing x corresponding to an expansion of the unit cell by 0.5–1% when compared to Mn_5Si_3 (ref. 2). The lattice constants were obtained by a least-squares fit of the Mn_5Si_3 structure to the measured lattice-plane distances: $a = 6.907$ Å, $c = 4.800$ Å for Mn_5Si_3 ; $a = 6.939$ Å, $c = 4.831$ Å for $Mn_5Si_3C_{0.8}$. The distortion of the Mn_{II} octahedra by carbon is anisotropic as inferred from the extended X-ray absorption fine-structure (EXAFS)². An anisotropic distortion of the Mn_5Si_3 -type structure by carbon was also reported for isostructural $Ti_5Si_3C_{0.47}$ compounds.¹⁰ This result strongly suggests that the carbon is not an ‘inert’

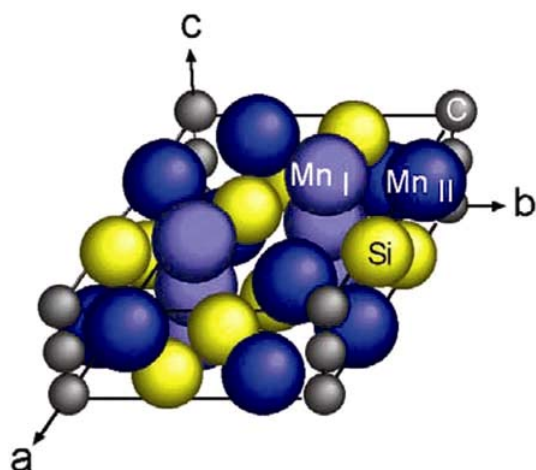


Figure 1. Hexagonal uni-cell of the Mn_5Si_3 -type structure with Mn located at two inequivalent Mn sites (Mn_I and Mn_{II}) and carbon arranged along chains through the center of Mn_{II} octahedra.

interstitial atom but participates in the chemical bonding to Mn.

The Nowotny phase is also formed in $Mn_5Ge_3C_{0.8}$ films. However, in this case the lattice parameters determined from the diffraction lines indicate a lattice compression caused by the incorporation of C⁵. For $x = 0.8$ we find $c = 4.996$ Å, $a = 7.135$ Å and $c/a = 0.700$, i.e. a compression in each direction when compared to $c = 5.053$ Å, $a = 7.184$ Å, $c/a = 0.703$ for Mn_5Ge_3 (ref. 11). This is in strong contrast to $Mn_5Si_3C_x$ films^{2,3} and $Mn_5Si_3C_x$ annealed powder samples¹ ($x \ll 1$), where the c/a ratio increases slightly upon interstitial insertion of carbon.

The magnetic structure of the carbon-free Mn_5Si_3 has been studied intensely.¹² Mn_5Si_3 has two antiferromagnetic (AF) phases, AF2 between the Néel temperatures $T_{N2} = 99$ K and $T_{N1} = 66$ K and AF1 below T_{N1} . The onset of long-range antiferromagnetic order at T_{N2} is accompanied by an orthorhombic distortion. The Mn atoms at two inequivalent sites, Mn_I and Mn_{II} , have different local magnetic moments resulting in a complicated magnetic structure which is highly non-collinear below T_{N1} . Figure 2 shows the temperature dependence of the magnetization $M(T)$ of the C-doped $Mn_5Si_3C_{0.8}$ films acquired with a superconducting interference-device in a weak magnetic field $\mu_0 H = 2.5$ mT applied parallel to the surface. The incorporation of carbon into the antiferromagnetic Mn_5Si_3 compound gives rise to a ferromagnetic magnetization curve and a Curie temperature $T_C = 352$ K for sputtered $Mn_5Si_3C_{0.8}$. The alloy film obtained by C implantation shows a similar $M(T)$ behaviour as the sputtered reference sample

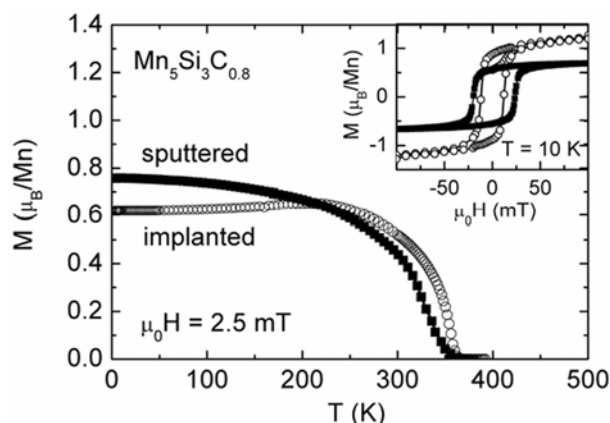


Figure 2. Magnetization $M(T)$ of magnetron sputtered (closed symbols) and C^+ -ion implanted (open circles) $Mn_5Si_3C_{0.8}$ films. Insets show $M(H)$ loops taken at $T = 10$ K.

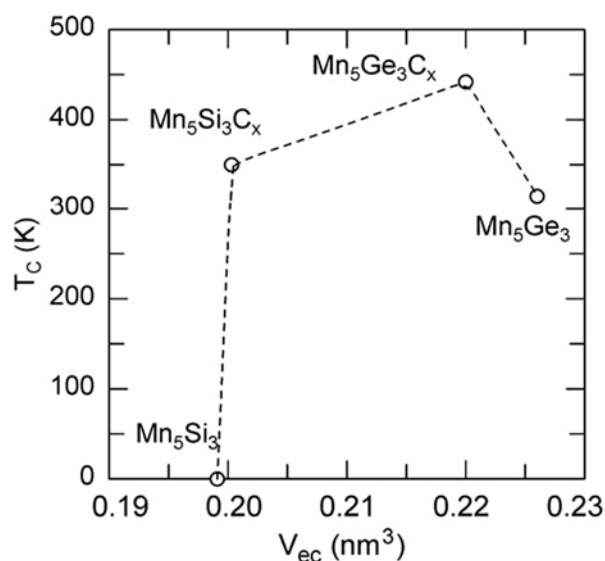


Figure 3. Curie temperatures of Mn_5Si_3 (antiferromagnetic, $T_C = 0$), $Mn_5Si_3C_{0.8}$, $Mn_5Ge_3C_{0.8}$, and Mn_5Ge_3 vs volume of the hexagonal unit-cell.

but with a reduced magnetization for $T < 200$ K. We mention that $M(T)$ of the C-implanted film was recorded after demagnetization of the system in contrast to the data of the sputtered film which were recorded after the film was magnetized in a high field. This explains the reduction of $M(T)$ for the implanted film at temperatures $T < 200$ K with respect to sputtered $Mn_5Si_3C_{0.8}$. A contribution from minor antiferromagnetic Mn–Si–C phases in the implanted film that reduce the total measured magnetization at low temperatures may also play a role. However, both $Mn_5Si_3C_{0.8}$ films show the same saturated magnetic moment $m_S \approx 1 \mu_B/Mn$, see the $M(H)$ loops in the inset of figure 2.

Using ion implantation allows a patterning of the films and a lateral modification of characteristic magnetic properties like the interlayer exchange coupling, the exchange bias effect, the magnetic damping behaviour, and the saturation magnetization.¹³ We only mention that in the present case the films were patterned by ion-implantation through a Au stencil mask to chemically modify the samples and to obtain C-doped regions that are embedded into the carbon-free host resulting in a lateral modification of magnetic order on the micrometer scale.⁶

For sputtered as well as for C-implanted $Mn_5Ge_3C_{0.8}$ films (not shown) a similar behaviour as for $Mn_5Si_3C_{0.8}$ was observed. In both $Mn_5Ge_3C_{0.8}$ films,

$T_C = 420$ – 450 K is strongly enhanced when compared to $T_C = 304$ K of carbon-free Mn_5Ge_3 (ref. 4). At $T = 10$ K, the average saturated moment $m_S = 2.2 \mu_B/Mn$ of the C-implanted samples is somewhat smaller than $2.6 \mu_B/Mn$ of Mn_5Ge_3 polycrystals.¹⁴ m_S is in good agreement with an average moment estimated from an empirical model, where the individual Mn moments in Mn_5X_3 ($X = Si, Ge$) compounds strongly depend on the different Mn–Mn bond lengths. From neutron-diffraction data, Forsyth and Brown presented evidence that the moment reduction at different Mn sites with respect to the free-ion value is governed by the nearest-neighbour Mn–Mn interaction.¹⁵ Below a critical average Mn–Mn bond length of about 3.1 \AA , each Mn neighbour reduces the moment of the coordinated Mn atom from the ionic value by about $2 \mu_B/\text{\AA}$. Applying this empirical relationship to the present samples, an average magnetic moment of about $2.3 \mu_B/Mn$ is expected for $Mn_5Ge_3C_{0.8}$.

From the measured structural and magnetic properties we obtain a relationship between T_C and the unit-cell volume V_{ec} , plotted in figure 3. The higher T_C obtained for $Mn_5Ge_3C_{0.8}$ compared to $Mn_5Si_3C_{0.8}$ is in agreement with the magnetic properties of bulk $Mn_5(Ge_{1-y}Si_y)_3$ alloys for which T_C increases monotonically with decreasing Si concentration $y \leq 0.75$, where the samples show a ferromagnetic behaviour.¹⁶ This is presumably due to the different electronic configuration of the metalloid atoms. The nonmonotonic behaviour shown in figure 3 further demonstrates that the enhanced Curie temperature of the carbon-doped compounds cannot be simply explained by a volume effect but arises from a combined effect of interstitial carbon atoms on the different interatomic distances and on the electronic structure.

4. Conclusion

In conclusion, $Mn_5Si_3C_{0.8}$ and $Mn_5Ge_3C_{0.8}$ films showing ferromagnetic properties with Curie temperatures well above room temperature can be obtained by co-sputtering or by C^+ -ion implantation. The different effect of carbon on the lattice parameters in $Mn_5Si_3C_{0.8}$ and $Mn_5Ge_3C_{0.8}$ suggest an additional effect of carbon on the electronic bonding. However, a detailed understanding of the relation between the structural and magnetic properties in these compound films awaits future electronic band-structure calculations.

Acknowledgements

Financial support from the DFG Center for Functional Nanostructures is gratefully acknowledged.

References

1. Sénateur J P, Bouchaud J-P and Fruchart R 1967 *Bull. Soc. Fr. Mineral. Cristallogr.* **90** 537
2. Sürgers C, Gajdzik M, Fischer G von, Löhneysen H, Welter E and Attenkofer K 2003 *Phys. Rev.* **B68** 174423
3. Gopalakrishnan B, Sürgers C, Montbrun R, Singh A, Uhlarz M and von Löhneysen H 2008 *Phys. Rev.* **B77** 104414
4. Tawara Y and Sato K 1963 *J. Phys. Soc. Jap.* **18** 773
5. Gajdzik M, Sürgers C, Kelemen M and von Löhneysen H 2000 *J. Magn. Magn. Mater.* **221** 248
6. Sürgers C, Potzger K, Strache T, Möller W, Fischer G, Joshi N and von Löhneysen H 2008 *Appl. Phys. Lett.* **93** 062503
7. Zeng C, Erwin S C, Feldman L C, Li A P, Jin R, Song Y, Thompson J R and Weitering H H 2003 *Appl. Phys. Lett.* **83** 5002
8. Corbett J D, Garcia E, Guloy A M, Hurng W-M, Kwon Y-U and Leon-Escamilla E A 1998 *Chem. Mater.* **10** 2824
9. Shah K V, Joshi Devang A, Manfrinetti P, Wrubl F, and Dhar S K 2007 *Proceedings of the DAE solid state physics symposium* (Mysore, India)
10. Williams J J, Kramer M J, Akinc M and Malik S K 2000 *J. Mater. Res.* **15** 1773
11. Castelliz L 1953 *Monatsh. Chem.* **84** 765
12. Silva M R, Brown P J and Forsyth J B 2002 *J. Phys.: Condens. Matter* **14** 8707 and references therein
13. Fassbender J and McCord J 2008 *J. Magn. Magn. Mater.* **320** 579
14. Kappel G, Fischer G and Jaéglé A 1973 *Phys. Lett.* **A45** 267
15. Forsyth B and Brown P J 1990 *J. Phys.: Condens. Matter* **2** 2713
16. Kappel G, Fischer G and Jaéglé A 1976 *Phys. Stat. Sol. (a)* **34** 691